2022 IEEE/ASME International Conference on
Advanced Intelligent Mechatronics (AIM)

Iterative Learning Control for the Active Error Correction of Polygon Mirror Based Laser Scanning

Bo Cong, Johannes Schlarp and Georg Schitter

2022 IEEE/ASME International Conference on Advanced Intelligent Mechatronics (AIM) | 978-1-6654-1308-4/22/$31.00 ©2022 IEEE | DOI: 10.1109/AIM52237.2022.9863305

***Abstract*—Polygon mirror (PM) based scanners suffer from scan line wobbles caused by facet variant pyramidal errors. The active error correction method uses a fast steering mirror (FSM) to adjust the laser reflection angle actively such that the wobble error can be compensated on the scan surface. This method requires the FSM to follow a fast varying and repetitive reference, which is challenging for the traditional feedback and feedforward control due to limited dynamic bandwidth and model accuracy. This paper proposes to use iterative learning control (ILC) for controlling the FSM, which significantly improves the correction effectiveness and reduces the line wobble for PM scanning systems.**

I. INTRODUCTION

Laser scanners are widely used in multiple industry processes, such as laser cutting, laser engraving and 3D printing. As the demand for high throughput and accuracy rises in industries, continuing research [1]–[5] has been conducted to develop laser scanners with large scan angle, fast scan speed while maintaining a high scanning accuracy. Among all the scanning technologies, the galvanometer [2][3], fast steering mirror (FSM) [4] and polygon mirror (PM) [5] are the most commonly used technologies.

Galvanometer scanners employ electromagnetic torque to rotate the permanent magnet shaft which is connected to a reflection mirror. This type of scanner can provide scanning angle to a tens of degrees, but typical with a scan rate less than 300 Hz [3]. Resonant scanners can overcome this limitation by oscillating at the resonance frequency [6]. However, this leads to a varying scan speed, giving a non-uniform resolution on scanning patterns. An FSM enables two dimensional fast scanning by utilizing flexure support systems [7]. This allows FSM to be operated with a bandwidth more than 1 kHz, but only within the range of a few degrees [4].

Polygon mirror based scanners generate scanning motion by spinning only in a single direction with constant speed. Since no dynamic motion is directly involved in the operation, the scan rate can exceed 10 kHz. Depending on the facet numbers, PM scanners can achieve a scanning angle from a few degrees to tens of degrees.

PM scanners have a wide scan range and high scan speed, but its scan accuracy is susceptible to manufacture imperfections [2]. The facet pyramidal errors from manufacturing process creates line wobbles which deteriorates the scanning accuracy [1][2]. The line wobble effects can be reduced by either passive or active corrections. The passive method employs a serial of optics, which first focuses the input laser beam in the cross-scan direction to the deflecting polygon facet, and then refocuses the laser to its original form after the deflection. This method can largely reduce the wobble effect from the pyramidal error in scanning. It is however limited by pupil shifting and optical qualities [8]. The active method compensates the pyramidal angle by pre-deflecting the laser beam using an optical steering mirror, thus eliminating the line wobble during scanning [9]. Since the polygon scanner is scanning at rate up to tens of kHz, this active method requires a fast trajectory tracking from the steering mirror. However, this requirement is not always feasible, due to dynamic bandwidth limitation [9][10]. Since the pyramidal error caused scan line wobble is determined by the PM and repeated after each PM revolution, the active correction is a repetitive reference tracking task. The learning control methods have shown great potential to improve tracking accuracy for repetitive references in various applications, such as in printers [11][12] and microscopies [13][14].

The contribution of this paper is to apply iterative learning control (ILC) to a polygon mirror based laser scanning system with active compensation by means of an FSM, improving scanning accuracy while maintaining fast scanning speed. The content of this paper is organized as follows. In Section II, the scan line wobble from polygon mirror based scanners is explained and the reference trajectory for active correction is demonstrated. Next, in Section III, the active correction is evaluated dynamically and the control challenge is illustrated. The basic feedback and feedforward control are explained in Section IV, and the proposed ILC control is designed in Section V. Experiment validation of proposed approach is presented in Section VI. Finally, Section VII concludes the paper.

II. SYSTEM DESCRIPTION

A. Polygon Scanner

In a typical PM based scanning system, the polygon mirror is rotated to reflect the scanning laser beams onto the scan surface, creating scan lines according to the given reference. Two-dimensional scanning is realized by shifting the relative position between the scan surface and the scanner head in the cross-scan direction. Typical scan errors of the PM scanner include facet to facet angle error α and pyramidal error θ, as indicated in Fig.1.

A geometrically perfectly shaped polygon have the facet-to-facet angle equal to 360°/N, where N is the number of facets. However, in industrial standard polygon mirrors, the facet-to-facet angle can deviate from the nominal value by 25 to 150 μrad, due to manufacturing imperfections [1]. This angle

The authors are with the Advance Mechatronic System group at the Automation and Control Institute, Technische Universität Wien, A-1040 Vienna, Austria. Corresponding author email: cong@acin.tuwien.ac.at

Published version of the article: Bo Cong, Johannes Schlarp and Georg Schitter, "Iterative Learning Control for the Active Error Correction of Polygon Mirror Based Laser Scanning," *Proceedings of 2022 IEEE/ASME International Conference on Advanced Intelligent Mechatronics (AIM)* pp. 522–527, 2022. DOI: 10.1109/AIM52237.2022.9863305

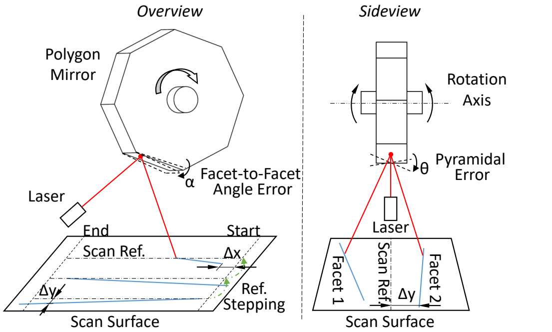

Fig. 1: PM based scanner. The scanning laser beam (solid red) is directed to the scan surface (solid blue) following the reference (dash-dot black). The polygon mirror has: facet-to-facet angle errors α and pyramidal errors θ such that the scan lines deviate from the reference. The deviations are indicated by Δx and Δy, respectively.

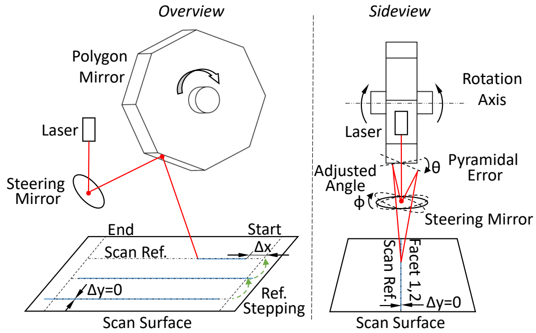

Fig. 2: PM based scanner with active correction. A steering mirror is introduced to the scanning systems that can actively adjust the reflection angle ϕ to correct the wobble error Δy, caused by the pyramidal error θ from the PM.

even varies per facet, resulting in different start positions for scanning lines, shown as Δx in Fig.1. This shift can commonly be solved by implementing a start of scan sensor [15], and will not be covered in this paper.

The pyramidal error describes the misalignment between the facet surface and the rotation axis. Ideally, the surface is in parallel to the axis and any variance will deviate the scan line away from its reference, shown by Δy in Fig.1. Typically, the pyramidal error differs per facet, within the range of 10 to 300 μrad [1]. As described in Section I, the pyramidal error will lead to line wobbles if no correction is implemented in the scanner.

The active correction method is shown in Fig.2, where a steering mirror is employed to direct the laser beam according to the pyramidal error of each facet, hence correcting the scan error. This method is not trivial, because even a constant pyramidal error θ requires a position varying steering angle $\phi(x)$ for compensation. This challenge is further investigated at an experimental PM scanner setup.

B. Setup Description

The PM scanner setup is shown in Fig.3, which consists primarily of a laser module (type: PhoxX-405-300, Omicron Laserage Laserprodukte GmbH, Germany) with 405 nm wavelength, a fast steering mirror (type: OIM101, Optics In Motion LLC, USA) with a one inch aperture, and a polygon mirror (type: PLS-08-525-125-AL-7.5K, Precision Laser Scanning LLC, USA) with 8 facets and 144 mm diameter.

The laser is initially deflected 70° by the FSM, and subsequently deflected by the rotating polygon to conduct scanning. During the rotation, approximately 50% of the rotation angle, where the laser is not split onto two adjacent facet, can be used for scanning. This gives an optical scan angle of ±21.8°. At a distance of 0.5 m between the scanner and the sample, a line speed of 500 m/s is achieved.

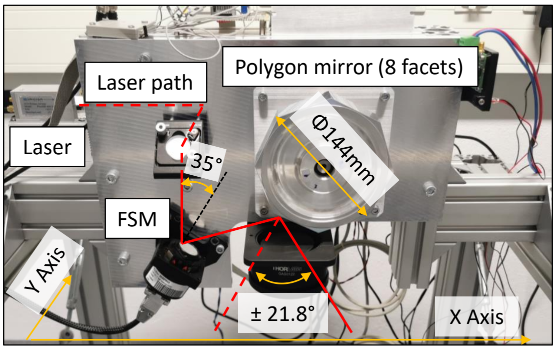

Fig. 3: Experimental PM scanner. The scanner operates at the maximum scanning speed of 1000 lines/s, with an optical scan angle of ±21.8°.

C. Scanning Sensitivity

Given the dimension and geometry of the scanner design, the scan line position can be computed, as well as its sensitivity to different optical parameters. Assuming that the scan reference is $y = 0$, the line wobbles caused by the PM pyramidal error on the sample is expressed by $y_{wob} = f(x_s, \theta)$ and the position correction yielded from the FSM adjustment is described by $y_{corr} = g(x_s, \phi)$, in which x_s is the laser position in scan direction on the sample, θ is the facet pyramidal error and ϕ is the FSM adjustment angle.

The y_{wob} and y_{corr} are visualized in Fig.4a for different angles of θ and ϕ. The sensitivities show a classic bowl shape of scanning, which is also identified in literatures [1], with a magnitude of approximately 1 μm/μrad. Using the FSM to actively compensate the line wobble requires to find a reference trajectory for ϕ such that

$$y_{wob} + y_{corr} = 0 \tag{1}$$

at each position x_s. The difference between sensitivities $f(x_s, \theta)$ and $g(x_s, \phi)$ indicates that the reference will not be

Published version of the article: Bo Cong, Johannes Schlarp and Georg Schitter, "Iterative Learning Control for the Active Error Correction of Polygon Mirror Based Laser Scanning," *Proceedings of 2022 IEEE/ASME International Conference on Advanced Intelligent Mechatronics (AIM)* pp. 522–527, 2022. DOI: 10.1109/AIM52237.2022.9863305

a trivial constant setpoint, but possibly a curved and position dependant trajectory $\phi = h(\theta, x_s)$.

Converting the position x_s to the corresponding optical scan angle, the reference trajectory is valid for any distance between the scanner and the sample. The resulting reference trajectories are depicted in Fig.4b.

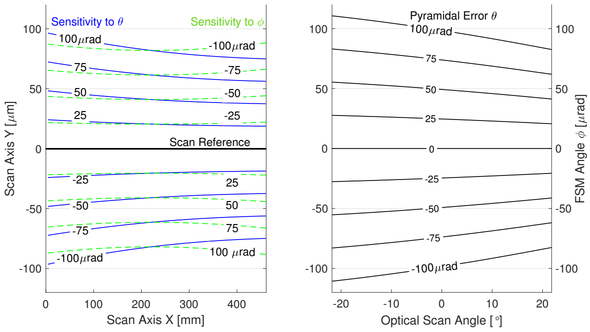

(a) Scan line position sensitivity (b) Reference trajectory

Fig. 4: (a) Line position resulted from various θ (solid blue lines) and ϕ (dashed green lines). Both sensitivities are curved, but with different orientations. (b) The calculated reference trajectory for the FSM adjustment angle ϕ as a function of the pyramidal error and the optical scan angle.

III. System Analysis and Dynamics

From the sensitivity study, a reference trajectory can be derived for the pyramidal error measured from the PM, where the angle of the steering mirror is coupled with the optical scan angle. The active correction is, however, not a static method, since the optical scan angle is matched with the PM rotation in time. In this section, the analysis reveals the dynamic challenges of the active correction method.

A. Scanning Characteristics

The PM scanner setup scans the samples with a rate of 1000 lines/s. To achieve active correction for this system, the FSM needs to follow and track curved trajectories timely and accurately within millisecond. Any deviation to the reference is seen as residual pyramidal errors, contributing to the line wobble with a sensitivity of approximately 1 μm/μrad as demonstrated in Fig.4a. The error tolerance for the scanning system is defined as 1/10 of the laser diameter, which is equivalent to 2.5 μm for the experimental setup and 2.5 μrad for the active correction.

Moreover, the reference is also not continuous by default. For every PM revolution, the eight polygon facets are involved consecutively to generate the scan lines. As the pyramidal errors varies per facet, the correction reference for each facet is spatially separated. To ensure that the active correction is effective throughout the entire revolution, the FSM has to jump between these separated trajectories during the transition between adjacent facets, and this typically requires high dynamic bandwidth. A spline interpolation is used to interconnect the scattered trajectories, while keeping the high-frequent components at a minimum.

For evaluation of the active correction, eight arbitrary angles within the variation of 50 μrad are assumed to be the pyramidal errors of the PM, which matches with [1]. Given the pyramidal errors, the required FSM reference is computed, and the resulted trajectory is shown in Fig.9.

As can be observed, the correction references for different facets are scattered with various orientations and shiftings, alternating in a rate of 2 kHz. To track this reference with a high accuracy ($\leq 1\%$), it typically requires the actuator to have a 7-10 times higher bandwidth [16]. However, state-of-the-art FSMs generally have a bandwidth of 1-2 kHz [7].

B. Fast Steering Mirror Identification

The FSM used in the setup is supported by a flexure that is compliant in two-degree of freedoms in a range of ± 26 mrad. The two rotational freedoms are decoupled [17], and only rotation ϕ is used for the scan wobble correction. The FSM rotation is sensed by an optical sensor attached on the back side of the mirror, with angular resolution of $\leq 2\mu$rad.

The system plant of the FSM is identified from the actuation current to the output mirror angle using multisine excitations, as shown in Fig.5. Note that a constant gain $K_0 = 0.089$ is applied to the excitation signals such that the input and output has the same unit in radiant. The first dynamic resonance of the plant is observed at 27 Hz, defined by the flexure stiffness and rotational inertia, and the structural dynamics only occur above 2 kHz. A time delay of t_d = 25 μs can be seen from the phase roll-off above 1 kHz.

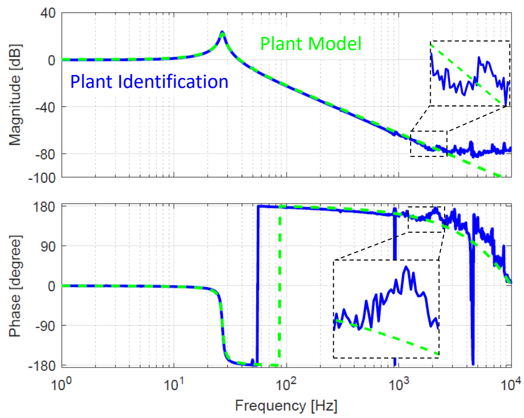

Fig. 5: Measured and modelled frequency response of the FSM in ϕ direction. The measured plant (solid blue) show multiple structural dynamics above 2 kHz. The modelled plant has the natural frequency resonance at 27 Hz (dashed green).

A simplified model $\hat{G}_{FSM}$ is created to describe the dominant dynamics of the FSM system. The model is expressed

Published version of the article: Bo Cong, Johannes Schlarp and Georg Schitter, "Iterative Learning Control for the Active Error Correction of Polygon Mirror Based Laser Scanning," *Proceedings of 2022 IEEE/ASME International Conference on Advanced Intelligent Mechatronics (AIM)*pp. 522–527, 2022. DOI: 10.1109/AIM52237.2022.9863305

by

$$\hat{G}_{FSM}(s) = \frac{\omega_0^2}{s^2 + 2\zeta\omega_0 \cdot s + \omega_0^2} \cdot e^{-s \cdot t_d}, \tag{2}$$

where $\omega_0 = 169.6$ rad/s is the flexure resonance frequency, $\zeta = 0.04$ is the damping ratio.

The achievable closed-loop bandwidth of the FSM is typically limited by its internal mode or structure dynamics [7]. In the case of the FSM from the setup, the maximum dynamic bandwidth would not exceed 2 kHz. A control system needs to be designed for the FSM such that it is able to track the fast varying correction reference.

IV. Feedback and Feedforward Control

Commonly feedback (FB) and feedforward (FF) control, as shown in Fig.6, is used to control the FSM. The design of the feedback controller C_{FB} and the feedforward controller C_{FF} is discussed in detail in this section.

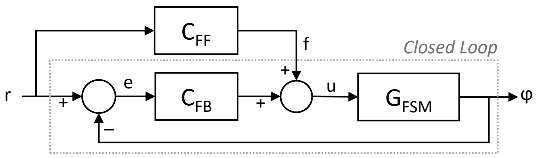

Fig. 6: General structure of implementing feedforward controller C_{FF} and feedback controller C_{FB}.

A. Feedback Control

For feedback control design, a standard PID controller with low-pass filter is used. The controller has the following form

$$C_{FB}(s) = K_P\left(1 + \frac{K_I}{s} + \frac{K_D s}{K_N s + 1}\right) \cdot \frac{\omega_{LP}^2}{s^2 + 2\pi\omega_{LP}s + \omega_{LP}^2} \tag{3}$$

with the PID parameters $K_P = 90$, $K_I = 10$, $K_D = 0.0016$ and $K_N = 8\times10^{-6}$ and the low-pass filter $\omega_{LP} = 6283$ rad. The integrator ensures zero steady state error tracking while the differentiator provides phase lead at the cross-over frequency of 800 Hz, securing 45° phase margin. The low-pass filter suppresses the dynamics above 2 kHz. The achieved closed loop bandwidth is approximately 1.2 kHz. Pushing the bandwidth higher ($\leq$ 2kHz) is at the cost of increasing the sensitivity to disturbances. This limitation is known in literature as waterbed effect for closed-loop sensitivity [18], which demonstrates the unavoidable trade-off between performance and robustness for feedback control.

B. Feedforward Control

As explained in the Section II and III, the reference trajectory, shown in Fig.4b, is pre-determined by the PM and the scanner design. Feedforward control is commonly used to improve tracking performance for a known trajectory.

Given the standard control framework shown in Fig.6, the tracking error can be derived by

$$e = S_{CL} \cdot r - G_{FSM} S_{CL} C_{FF} \cdot r, \tag{4}$$

where the S_{CL} is the closed-loop sensitivity. Since a single input single output system is considered, the ideal feedforward controller is simply

$$C_{FF} = G_{FSM}^{-1}. \tag{5}$$

However, the exact plant is hardly known in practice. Moreover, implementing the controller (5) can amplify high-frequency noises and excite unwanted internal models, hence disturbing the tracking performance. Alternatively, an approximate plant inverse

$$C_{FF} = \hat{G}_{FSM}^{-1} \cdot F_{BW} F_{BW}' \tag{6}$$

is designed for the feedforward controller, in which $\hat{G}_{FSM}^{-1}$ is the inverse model, F_{BW} is a 4^{th} order Butterworth filter with a cut-off frequency of 2 kHz, and F_{BW}' is the same Butterworth filter with inverse phase.

The performance of the FB and FF controlled FSM is shown in Fig.9, where the controlled system is unable to track the reference with micro-radiant accuracy. The implementation of the controllers and the experiment results are discussed in detail in Section VI.

V. Iterative Learning Control

Traditional model based control design (FB and FF) calculates the control output based on the knowledge of system plant, reference and disturbance. Due to the presence of unknown disturbance and model uncertainty in practice, the calculated control signal is mostly not optimal for achieving the desired tracking performance. This problem can be alleviated by adapting the control signal from previous errors, where the system is operated in repetitive fashion such as in the active correction for PM scanners.

The ILC is proposed to improve the performance of active correction by learning the optimal control signal through repetitive iterations. The standard learning structure, shown in Fig.7, is employed for the implementation, where j denotes the iteration number. Since the correction reference is repeated per PM revolution, any number of revolution can be regarded as r, which remains identical in each iteration.

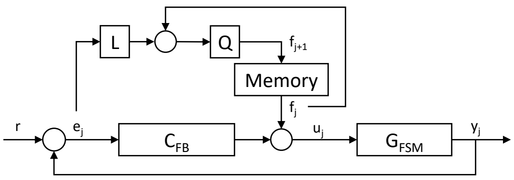

Fig. 7: ILC control structure. The feedforward output f_j is updated in every iteration in accordance to the measured error e_j and the learning filter L. The filter Q is tuned to ensure learning convergence.

Published version of the article: Bo Cong, Johannes Schlarp and Georg Schitter, "Iterative Learning Control for the Active Error Correction of Polygon Mirror Based Laser Scanning," *Proceedings of 2022 IEEE/ASME International Conference on Advanced Intelligent Mechatronics (AIM)*pp. 522–527, 2022. DOI: 10.1109/AIM52237.2022.9863305

Given the framework, Equation (7) and (8) can be derived, describing the update of the feedforward signal and the tracking error.

$$f_{j+1} = Q \cdot (L \cdot e_j + f_j) \tag{7}$$

$$e_{j+1} = Q \cdot (1 - G_{FSM} S_{CL} L) e_j + (1 - Q) \cdot S_{CL} r \tag{8}$$

The Equation (8) also defines the stability and performance of the ILC control [19]. The convergence of iterative learning is guaranteed if condition

$$|Q \cdot (1 - G_{FSM} S_{CL} L)| < 1 \tag{9}$$

is satisfied in the frequency range up to the Nyquist frequency [20]. If the learning converges, the end performance e_∞ is derived as

$$e_\infty = (1 - Q(1 - G_{FSM} S_{CL} L))^{-1} \cdot (1 - Q) \cdot e_1, \tag{10}$$

in which $e_1 = S_{CL} r$ is the tracking error in the first iteration.

To achieve the optimal performance while maintaining the learning convergence, the natural choice of the filters should be $L = S_{CL}^{-1} G_{FSM}^{-1}$ and $Q = 1$. However, the exact inverse plant and sensitivity are susceptible to the uncertainties in system identification, hence not used in practice. Instead, the modelled inverse system

$$L = \hat{S}_{CL}^{-1} \hat{G}_{FSM}^{-1} \tag{11}$$

is employed as the learning filter, in which $\hat{S}_{CL}$ is the modelled closed-loop sensitivity. Substituting (11) into (9) gives the following expression for the learning convergence criterion

$$\left| Q \cdot (1 - G_{FSM} S_{CL} \cdot \hat{S}_{CL}^{-1} \hat{G}_{FSM}^{-1}) \right| < 1. \tag{12}$$

The choice of the Q filter is consequently a trade off between pursuing optimal performance and ensuring learning convergence. Conclusions given in [14] suggest that $Q = 1$ can be maintained till the frequency range where the uncertainty and modelling error of the system dynamics exceed $\pm$ 90°. A commonly used form is selected for the Q filter

$$Q = F_{BW} F'_{BW}, \tag{13}$$

where F_{BW} is a 4^{th} order Butterworth filter, and F'_{BW} is the filter with inverse phase, making (13) a zero-phase filter. The cut-off frequency for F_{BW} is determined by evaluating Equation (12) with different Q choices, as shown in Fig.8.

As results, the cut-off frequency of 2 kHz is chosen for the filter Q, which fulfills the convergence criterion.

VI. Experiment Results and Discussion

The designed controllers are implemented on the FSM by a real-time data acquisition system (Type: DS1005, dSPACE GmbH, Germany) with sample frequency of 20 kHz. In the ILC implementation, one PM revolution is regarded as one iteration, and measures are taken to reduce performance impact from stochastic sensor noises, where an average $\bar{e}_j$ over 400 revolutions is taken for e_j. The achieved tracking performance from the designed controllers is shown in Fig.9.

The FB controlled system with a bandwidth of only 1.2 kHz is unable to follow the fast varying trajectory. A time lag of approximate 0.3 ms can be observed, resulting maximum 39 μrad tracking error. Clearly, a much higher bandwidth would be necessary to reduce the tracking error to micro-radiant level, if only the FB control is employed.

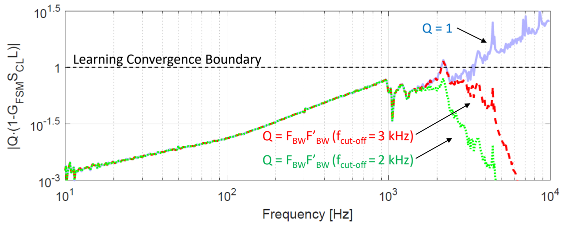

Fig. 8: ILC convergence analysis. Equation (12) is evaluated for different choices of the Q filter. The filter with $\leq$2 kHz cut-off frequency guarantees the learning convergence.

Adding the FF control prepares the FSM with upcoming dynamics beforehand, hence eliminating the time lag and improving the tracking performance. However, a maximum of 5.6 μrad tracking error still remains, due to the mismatch between the inverse model (6) and the inverse plant (5). This mismatch leads to an inaccurate FF output to the FSM, and this error is amplified by dynamic accelerations. As seen in Fig.9, the tracking error is significantly larger at the turns of the reference, where higher acceleration is needed from the FSM.

The ILC control reduces the tracking error further by adapting the control signal through iterations. The maximum tracking error is reduced to 1.3 μrad, which equals to approximately 1.3 μm position error on the scan sample. The learning process can be seen in Fig.10. After about five to six iterations, the RMS tracking error converges to the indicated value 0.48$\pm$0.02 μrad, hence the learning is stopped after 20 iterations. The end performance is limited by the cut-off frequency of the Q filter, which dictates the limits of learning dynamics. In order to learn higher frequent dynamics, and at the same time ensure the learning convergence, a more accurate model that includes structural dynamics is necessary.

In summary, the FB stabilized FSM with ILC control improves the correction effectiveness by a factor 4.5, compared to the FB and FF controlled system, and reduces the line wobble by factor 38, achieving a scanning accuracy $\leq$ 1.3 μm.

VII. Conclusion

In this paper, the ILC control was designed and implemented on the FSM to actively correct the line wobble of PM scanning systems. The pyramidal error of the PM is the main cause for the line wobble and varies per facet. The needed reference trajectory for the FSM is retrieved by analysing the sensitivity from the scan line position to the pyramidal error and to the adjustment angle. The reference varies at the scanning rate and repeats in each PM revolution. The FSM with only the FB controller is not able to provide effective correction for the PM line wobble due to bandwidth

Published version of the article: Bo Cong, Johannes Schlarp and Georg Schitter, "Iterative Learning Control for the Active Error Correction of Polygon Mirror Based Laser Scanning," *Proceedings of 2022 IEEE/ASME International Conference on Advanced Intelligent Mechatronics (AIM)* pp. 522–527, 2022. DOI: 10.1109/AIM52237.2022.9863305

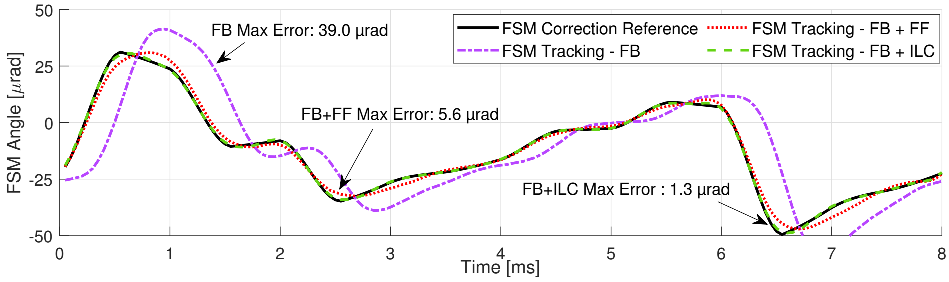

Fig. 9: Experiment results for FSM tracking performance. FSM tracks the correction angle reference (solid black) with different control structures. The maximum tracking errors are 39.0 μrad, 5.6 μrad and 1.3 μrad for FB controlled (dash-dotted purple), FB and FF controlled (dotted red), and FB and ILC controlled (dashed green) FSM respectively.

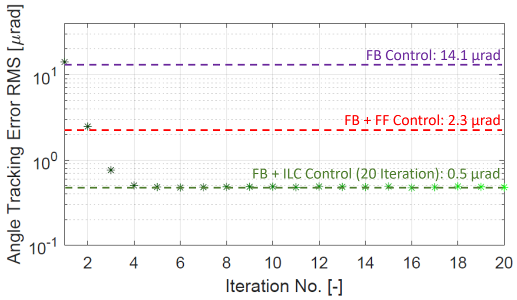

Fig. 10: ILC learning progress. The resulted RMS tracking error is plotted from each iteration, compared with the FB controlled (purple dashed line) and the FB and FB controlled (red dashed line) systems. The tracking error after 20 iterations is indicated by the green dashed line.

limitation. Adding a FF controller improves the correction effectiveness by a factor 6.5, but still a maximum of 5.6 μm of wobble error remains. The proposed ILC control adapting the control signal through repetitive iterations, improving the tracking performance by factors 30 and 4.5, compared to the FB controlled and the FB and FF controlled FSM. This improvement consequently increases the effectiveness of active correction for PM scanning systems, and achieves a scanning accuracy $\leq$ 1.3 μm.

ACKNOWLEDGMENT

The support from Cubicure GmbH and the financial support by the Austrian Research Promotion Agency (FFG) under project number 874705 are gratefully acknowledged.

REFERENCES

[1] G. F. Marshall and G. E. Stutz, Eds., *Handbook of Optical and Laser Scanning*. CRC Press, oct 2018.
[2] M. N. Sweeney, "Polygon scanners revisited," in *Optical Scanning Systems: Design and Applications*, L. Beiser and S. F. Sagan, Eds. SPIE, jul 1997.
[3] V.-F. Duma, K. sung Lee, P. Meemon, and J. P. Rolland, "Experimental investigations of the scanning functions of galvanometer-based scanners with applications in OCT," *Applied Optics*, vol. 50, no. 29, p. 5735, oct 2011.
[4] E. Csencsics, B. Sitz, and G. Schitter, "A fast piezo actuated tip/tilt mirror for raster scan applications," *IFAC-PapersOnLine*, vol. 52, no. 15, pp. 289–294, 2019.
[5] G. Stutz, "High speed printing with polygon scan heads," in *Components and Packaging for Laser Systems II*, A. L. Glebov and P. O. Leisher, Eds. SPIE, apr 2016.
[6] R. P. Aylward, "Advances and technologies of galvanometer-based optical scanners," in *Optical Scanning: Design and Application*, L. Beiser, S. F. Sagan, and G. F. Marshall, Eds. SPIE, jul 1999.
[7] E. Csencsics and G. Schitter, "Exploring the pareto fronts of actuation technologies for high performance mechatronic systems," *IEEE/ASME Transactions on Mechatronics*, vol. 26, no. 2, pp. 1053–1063, apr 2021.
[8] G. E. Stutz, "Eliminating laser scanner artifacts in binary and continuous-tone printing," in *Micro-Optics/Micromechanics and Laser Scanning and Shaping*. SPIE, may 1995.
[9] J. Wu and M.-H. Chu, "Wobble error correction for laser scanners," in *SPIE Proceedings*, A. G. Tescher, Ed. SPIE, dec 1986.
[10] M. N. Sweeney, G. A. Rynkowski, M. Ketabchi, and R. Crowley, "Design considerations for fast-steering mirrors (FSMs)," in *SPIE Proceedings*, S. F. Sagan, G. F. Marshall, and L. Beiser, Eds. SPIE, jun 2002.
[11] L. Blanken, J. Willems, S. Koekebakker, and T. Oomen, "Design techniques for multivariable ILC: Application to an industrial flatbed printer," *IFAC-PapersOnLine*, vol. 49, no. 21, pp. 213–221, 2016.
[12] H. W. Yoo, C. J. Kerschner, S. Ito, and G. Schitter, "Iterative learning control for laser scanning based micro 3d printing," *IFAC-PapersOnLine*, vol. 52, no. 15, pp. 169–174, 2019.
[13] J. A. Butterworth, L. Y. Pao, and D. Y. Abramovitch, "A comparison of ILC architectures for nanopositioners with applications to AFM raster tracking," in *Proceedings of the 2011 American Control Conference*. IEEE, jun 2011.
[14] H. W. Yoo, S. Ito, and G. Schitter, "High speed laser scanning microscopy by iterative learning control of a galvanometer scanner," *Control Engineering Practice*, vol. 50, pp. 12–21, may 2016.
[15] C. Rensch, S. Hell, M. v. Schickfus, and S. Hunklinger, "Laser scanner for direct writing lithography," *Applied Optics*, vol. 28, no. 17, p. 3754, sep 1989.
[16] R. Demerow, "Settling time of operational amplifiers," *Analog Dialogue*, 1970.
[17] E. Csencsics and G. Schitter, "System design and control of a resonant fast steering mirror for lissajous-based scanning," *IEEE/ASME Transactions on Mechatronics*, vol. 22, no. 5, pp. 1963–1972, oct 2017.
[18] G. Goodwin and M. Seron, "Fundamental design tradeoffs in filtering, prediction, and smoothing," *IEEE Transactions on Automatic Control*, vol. 42, no. 9, pp. 1240–1251, 1997.
[19] K. L. Moore, *Iterative learning control for deterministic systems*. Springer Science & Business Media, 2012.
[20] J. Chen and G. Gu, *Control-oriented system identification: an H∞ approach*. Wiley-Interscience, 2000.

Published version of the article: Bo Cong, Johannes Schlarp and Georg Schitter, "Iterative Learning Control for the Active Error Correction of Polygon Mirror Based Laser Scanning," *Proceedings of 2022 IEEE/ASME International Conference on Advanced Intelligent Mechatronics (AIM)*pp. 522–527, 2022. DOI: 10.1109/AIM52237.2022.9863305